The Meteoritical Society

Meteoritics & Planetary Science 44, Nr 7, 971–984 (2009)
Abstract available online at http://meteoritics.org

Tellurium isotope compositions of calcium-aluminum-rich inclusions

Manuela A. FEHR[1, 4*], Mark REHKÄMPER[2, 4], Alex N. HALLIDAY[3, 4], Bodo HATTENDORF[5], and Detlef GÜNTHER[5]

[1]Department of Earth and Environmental Sciences, The Open University, Milton Keynes MK7 6AA, UK
[2]Impact and Astromaterials Research Centre (IARC) and Department of Earth Science and Engineering, Imperial College, London, SW7 2AZ, UK
[3]Department of Earth Sciences, Oxford University, Oxford OXI 3PR, UK
[4]Institute of Isotope Geology and Mineral Resources, ETH Zürich, 8092 Zürich, Switzerland
[5]Laboratory of Inorganic Chemistry, ETH Zürich, 8093 Zürich, Switzerland
[*]Corresponding author. E-mail: M.A.Fehr@open.ac.uk
Present address: Department of Earth and Environmental Sciences, The Open University, Walton Hall, Milton Keynes MK7 6AA, UK

(Received 11 August 2008; revision accepted 02 May 2009)

Abstract–A method for the precise and accurate determination of the tellurium (Te) isotope compositions of calcium-aluminum-rich inclusions (CAIs) has been developed. The technique utilizes multiple-collector inductively coupled plasma-mass spectrometry (MC-ICPMS) with either Faraday detectors or a dual ion-counting system. The external reproducibility (2σ) for $^{126}Te/^{125}Te$ was ~15‰ and ~2‰ when 3 pg and 65 pg of Te were analyzed with the electron multipliers. Measurements performed on 200 pg of Te using Faraday detectors and time-resolved software displayed an external reproducibility of ~8‰ for $^{126}Te/^{124}Te$, whereas 3 ng Te could be measured to a precision of about 0.6‰.

Analyses of five CAIs from the Allende chondrite yielded Te concentrations that range from 12 to 537 ppb and the inclusions are therefore depleted in Te relative to bulk Allende by factors of about 2 to 86. The Sn/Te ratios of the CAIs are also fractionated compared to bulk Allende (which displays $^{124}Sn/^{128}Te \approx 0.1$) with $^{124}Sn/^{128}Te$ ratios of about 0.1 to 2.5. The Te isotope measurements for these refractory inclusions yielded no ^{126}Te excesses from the decay of the short-lived radionuclide ^{126}Sn ($\tau_{½}$ = 234,500 years) and the most precise analysis provided a $\varepsilon^{126}Te$ value of 1 ± 6 ($\varepsilon^{126}Te = {}^{126}Te/{}^{124}Te$ normalized to $^{122}Te/^{124}Te = 0.53594$ and reported relative to the JMC Te standard). Minor differences in the Te isotope composition of the CAIs relative to the terrestrial standard and bulk Allende hint at the presence of small deficits in *r*-process Te isotopes or excess of *s*-process Te, but these nucleosynthetic anomalies are barely resolvable given the analytical uncertainties. Hence, it is also conceivable that these effects reflect small unresolved analytical artifacts.

INTRODUCTION

The former presence of short-lived nuclides with half-lives of less than 1 Myr (e.g., ^{26}Al, ^{41}Ca) in meteorites requires that these isotopes were produced either within the nascent solar system by spallation or in a late stellar nucleosynthetic event that took place just prior to the collapse of the protosolar cloud (Lee et al. 1998; Meyer and Clayton 2000). The ^{126}Sn – ^{126}Te decay system ($\tau_{½}$ = 234,500 years) (Oberli et al. 1999) is of particular interest in this regard because radioactive ^{126}Sn cannot be generated in significant amounts by the *s*-process, due to the short half-life of ^{125}Sn (9.6 days). Nor can it be the product of spallation. It is therefore produced exclusively by the *r*-process, which is thought to occur mainly in supernova environments (Qian et al. 1998). The discovery of ^{126}Te excesses from the decay of ^{126}Sn therefore provides strong evidence for a supernova trigger for the formation of the solar system (Cameron and Truran 1977) and the aerogel-model (Ouellette et al. 2005), in which short-lived radionuclides from a supernova are injected into an already-formed protoplanetary disk (Chevalier 2000).

Tellurium is also well suited for the study of nucleosynthetic processes, as it has eight stable nuclides, which are a mixture of *p*-process, *s*-process and *r*-process components. Bulk chondrites and iron meteorites have the same Te isotope composition as the Earth (Fehr et al. 2005), whereas presolar diamonds from Allende are the host of large nucleosynthetic isotope anomalies of *r*-process Te isotopes

(Richter et al. 1998; Maas et al. 2001). Sequentially leached phases of carbonaceous chondrites furthermore hint at the potential presence of minor excesses in the abundances of ^{130}Te and ^{128}Te (Fehr et al. 2006). This is consistent with a small excess of an *r*-process component or an *s*-process deficit, even though the isotope variations are barely resolvable given the analytical uncertainties.

Calcium-aluminum-rich inclusions (CAIs) are the host of many isotope anomalies from the decay of short-lived radionuclides and nucleosynthetic processes (see Podosek and Swindle 1988; MacPherson 2003; McKeegan and Davis 2003; Birck 2004 and references therein). They are furthermore thought to be the first solids that formed in the solar system (Göpel et al. 1994; Amelin et al. 2002; Bouvier et al. 2007; Jacobsen et al. 2008). Hence, CAIs are ideal targets for investigations that seek to identify nucleosynthetic Te isotope anomalies and excesses in the abundance of ^{126}Te from the decay of the formerly live ^{126}Sn.

Tin and tellurium are both moderately volatile elements, and are therefore expected to be depleted in high-temperature condensates, such as CAIs. Some studies, however, have also identified CAIs that are enriched in the moderately and highly volatile elements, including Sn, Zn, and Cd (Grossman and Ganapathy 1976; Friedrich et al. 2005; Wombacher et al. 2008). These enrichments are generally thought to be the result of secondary alteration on a parent body and may therefore be unrelated to the formation of the condensates in the early solar nebula (Grossman and Ganapathy 1976; MacPherson 2003). This interpretation, however, is not in accord with recently published Zn and Cd stable isotope data for Allende CAIs, which suggest that the volatile element enrichments of some CAIs are related to reactions with a gas phase (Luck et al. 2005; Wombacher et al. 2008).

Mason and Martin (1977) reported Sn concentrations of up to 8 ppm in Allende CAIs, whereas bulk Allende has only 0.54 ppm Sn (Fehr et al. 2005). Furthermore, spinels, which are abundant minerals in CAIs, could potentially have high Sn/Te ratios, because Sn can be incorporated into the spinel structure (Bergerhoff et al. 1970). Such samples are of particular interest because the high Sn/Te ratios would facilitate the detection of anomalies in the abundance of ^{126}Te that are due to the decay of formerly live ^{126}Sn.

In the present study, we have modified and optimized recently published Te isotope measurement techniques (Fehr et al. 2004, 2006) that utilize multiple-collector inductively coupled plasma-mass spectrometry (MC-ICPMS) for analyses of very small amounts of Te extracted from CAIs. The most important difference is that we use electron multipliers for the Te isotope measurements. These new procedures enabled the acquisition of Te isotope data for five CAIs from the carbonaceous chondrite Allende.

PREPARATION OF SAMPLES

Three samples were extracted from a single piece of the Allende carbonaceous chondrite (USNM 3937) using metal tools and plastic tweezers: (i) 16 mg of material from several individual CAIs (USNM 3937 A), (ii) a Fluffy Type A CAI of 4.3 mg (USNM 3937 B), and (iii) a spinel-rich inclusion of 10.5 mg (USNM 3937 C). Furthermore, two coarse-grained refractory inclusions from Allende, which were previously characterized and analyzed for their Sn content by Mason and Martin (1977), were provided by the Smithsonian Institution: USNM 5171 (33 mg) and USNM 3529 G (27.3 mg).

ANALYTICAL METHODS

Chemical Procedures

The three CAIs from sample USNM 3937 were sequentially treated with acids of increasing strength in order to remove potential metal contamination from extraction tools and to chemically separate sulfides, silicates, and spinels (Table 1). After each treatment, the samples were centrifuged and the supernatant was removed with a pipette. A mild 0.5 M HCl or 2 M HCl leach was applied first, to remove any metal contamination from the extraction tools as well as the sawed surface from which the Fluffy Type A CAI was sampled, and adhering sulfides from the chondrite matrix. Sample USNM 3937 A was additionally treated with HNO_3-Br_2 to release further sulfide phases. In the last two leach steps (Table 1), silicates were first leached with 15 M HF, and more acid resistant phases, such as spinels, were then completely digested with concentrated HF-HNO_3 in a Teflon bomb with steel jacket. Samples USNM 5171 and USNM 3529 G were also digested in a Teflon bomb with steel jacket but without prior leaching.

Tellurium was chemically separated from the CAI matrix using a two-stage column chemistry procedure described in detail by Fehr et al. (2004). The first separation step was scaled-down for smaller sample volumes, using anion-exchange columns with 100 µl of resin (Bio Rad AG1 X 8, 200–400 mesh). Samples were loaded in 300 µl 5 M HF. After elution of matrix elements with 675 µl 5 M HF, 300 µl 15 M HF and 600 µl 6 M HCl, Te and Sn were collected using 500 µl 1 M HNO_3. The second separation step utilized 200 µl Eichrom Tru-Spec™ resin. Samples were loaded in 1 ml 0.5 M HCl and Te was collected with 5 ml of 0.5 M HCl. The combined Te yield of this separation procedure is about 70%.

Mass Spectrometry

The Te isotopic measurements were performed with a Nu Plasma MC-ICPMS instrument at the ETH Zürich.

Table 1. Leach procedure used for the CAI samples.

Step	Reagent	Procedure	Sample
1a	0.5 M HCl	1 hour, RT	USNM 3937 A
1b	2 M HCl	1 day, RT	USNM 3937 B + C
2	HNO_3-Br_2[a]	14 hours, 60 °C	USNM 3937 A
3	15 M HF	1 day, 100 °C	All USNM 3937
4	Concentrated HF-HNO_3	4 days, 170 °C, steel bomb	All

[a]Mixture of 0.75 ml 2.7 M HNO_3 and 0.25 ml bromine water. Saturated bromine water was prepared as described by Rehkämper and Halliday (1999).
RT = room temperature.

Measurements with Faraday Collectors

Samples that contained more than ~100 pg Te were measured by static multiple collection using Faraday collectors with procedures similar to those described by Fehr and co-workers (Fehr et al. 2004, 2006). Data acquisition for the HNO_3-Br_2 leach of sample USNM 3937 A used a standard protocol that involved 20 data collection cycles of 5 s each. All other analyses utilized the time-resolved software of the instrument, which was originally developed for laser-ablation measurements. This permits the measurement of small quantities of Te with a short signal of high intensity (4–33 ppb Te). For very small samples (USNM 3529 G, 3937 B 15 M HF leach, 5171), the application of the time-resolved software is preferable to the standard procedures because it optimizes the time spent on data acquisition.

The measured Te isotope ratios were normalized to $^{122}Te/^{124}Te = 0.53594$ (Lee and Halliday 1995) with the exponential law to correct for mass fractionation. The $\varepsilon^{x}Te_{24}$ values of the samples were calculated relative to the mean results obtained for a JMC Te standard solution of similar concentration measured on the same day, using $\varepsilon^{x}Te_{24} = \{[(^{x}Te/^{124}Te)_{24\ sample} - (^{x}Te/^{124}Te)_{24\ std}]/(^{x}Te/^{124}Te)_{24\ std}\} \times 10^4$. The $\varepsilon^{x}Te_{56}$ data of the samples were determined in a similar manner, following internal normalization of the measured isotope ratios to $^{125}Te/^{126}Te = 0.374902$ (Lee and Halliday 1995) and using $\varepsilon^{x}Te_{56} = \{[(^{x}Te/^{125}Te)_{56\ sample} - (^{x}Te/^{125}Te)_{56\ std}]/ (^{x}Te/^{125}Te)_{56\ std}\} \times 10^4$. The reproducibility (2s) of the isotopic data for a Te standard solution with matching concentration provided a conservative estimate for the 2σ uncertainties of the sample analyses. The analytical uncertainties reported for samples (Table 2 and 3, Figs. 2–4) include the uncertainties of the sample and the standard measurement, which were combined using $\sigma = \sqrt{(\sigma_{sample}^2 + \sigma_{std}^2)}$.

Measurements with Electron Multipliers

The mass-spectrometric procedures of Fehr et al. (2004) were significantly modified for the determination of Te isotope compositions on <100 pg of Te. In this case, the analyses utilized a dual ion counting system, but this restricted the data collection to $^{126}Te/^{125}Te$. In order to prevent rapid deterioration of the electron multipliers, the Te signals were restricted to less than 100,000 counts/s. This limited the amount of Te that could be analyzed with this technique during a certain time.

Standard and sample measurements each comprised the acquisition of 40 isotope ratios with 5 s integrations. After each run, a wash cycle was performed, during which 0.1 M HNO_3, 1 M HNO_3 and 0.1 M HNO_3 were each aspirated for 1 min. On-peak background measurements were carried out for 5 minutes prior to and after each standard and sample run. This permits a precise offline interference correction for the ^{126}Xe that is present in the Ar-plasma gas. No mass-bias correction or additional interference corrections were applied to the data.

The $\varepsilon^{126/125}Te_M$ (M: measured) values were calculated from these results using the sample standard bracketing technique, whereby the sample data were referenced to the mean of the preceding and succeeding JMC Te measurements: $\varepsilon^{126/125}Te_M = \{[(^{126}Te/^{125}Te)_{M\ sample} - (^{126}Te/^{125}Te)_{M\ std\ mean}]/ (^{126}Te/^{125}Te)_{M\ std\ mean}\} \times 10^4$. The reproducibility (2s) of the isotope data for a Te standard solution with matching concentration was used as a conservative estimate for the 2σ uncertainty of the sample results. The analytical uncertainties reported for samples (Table 2, Fig. 2) include the uncertainties of the sample and the standard measurement, which were combined using $\sigma = \sqrt{(\sigma_{sample}^2 + \sigma_{std}^2)}$.

Concentration Measurements and Blanks

The Sn and Te concentrations of sample USNM 3937 A were measured by quadrupole ICP-MS (Agilent 7500cs) at the ETH Zürich on sample solution aliquots that did not undergo chemical separation, to avoid any chemical fractionation of Sn from Te. The concentrations were determined after external calibration, using synthetic standard solutions, and Rh and Cd were used as internal standards to compensate for non-spectral interferences. Both samples and standards were prepared in 0.5 M HNO_3 and 0.01 M HF to stabilize Sn and Te and prevent precipitation of SnO_2. Each digested sample was diluted to a concentration of below 1‰ of the original sample. The limits of detection (LODs) were 0.01 ppb for ^{118}Sn and 0.025 ppb for ^{125}Te, which corresponds to abundances of about 10 ppb Sn and 30 ppb Te for the original samples, depending on the final dilution. The Sn, Te, and Sn/Te data have large uncertainties due to concentrations close to the LOD and the blank contribution. The blanks for Sn (0.4–0.5 ng) were directly subtracted from the data. The Sn blank contribution is 81% for the steel bomb digestion and 18–26% for the other leach fractions. Blanks for Te concentration measurements are at or below the detection limit, corresponding to 0.7–1.1 ng Te, which thus defines the

Table 2. Te isotope data of Allende CAIs and CAI matrix test samples normalized to $^{122}Te/^{124}Te$.

Sample	Description	Leach/bulk	Weight (mg)	$\varepsilon^{120}Te_{24} \pm 2\sigma$	$\varepsilon^{125}Te_{24} \pm 2\sigma$	$\varepsilon^{126}Te_{24} \pm 2\sigma$	$\varepsilon^{126/125}Te_{M}$ [a] $\pm 2\sigma$	$\varepsilon^{128}Te_{24} \pm 2\sigma$	$\varepsilon^{130}Te_{24} \pm 2\sigma$
Allende CAIs									
USNM 3529 G[b]	Coarse-grained CAI, group I	Bulk	27.3	144 ± 265	5.0 ± 5.2	1.0 ± 6.0		0 ± 12	1 ± 18
USNM 3529 G	Coarse-grained CAI, group I	Bulk		−104 ± 243	0 ± 15	−6 ± 20		−9 ± 35	−16 ± 51
USNM 3937 A	Several CAIs	HNO_3-Br leach	16.0	1037 ± 2704	11 ± 50	21 ± 87		28 ± 153	36 ± 220
USNM 3937 A	Several CAIs	HNO_3-Br leach					−21 ± 23		
USNM 3937 A	Several CAIs	HNO_3-Br leach					60 ± 175		
USNM 3937 B	Fluffy Type A	2 M HCl leach	4.3				−3 ± 63		
USNM 3937 B[c]	Fluffy Type A	15 M HF leach		150 ± 2598	−4 ± 40	0 ± 81		−12 ± 149	
USNM 3937 B	Fluffy Type A	Steel bomb					−11 ± 84		
USNM 3937 C	Spinel-rich inclusion	2 M HCl leach	10.5				−79 ± 110		
USNM 3937 C	Spinel-rich inclusion	2 M HCl leach					0 ± 90		
USNM 3937 C	Spinel-rich inclusion	15 M HF leach					29 ± 45		
USNM 3937 C	Spinel-rich inclusion	Steel bomb					137 ± 287		
USNM 3937 C	Spinel rich inclusion	Steel bomb					11 ± 129		
USNM 5171[b]	Coarse-grained CAI, group I	Bulk	33.0	207 ± 552	2 ± 21	−13 ± 24		−21 ± 39	−30 ± 55
USNM 5171	Coarse-grained CAI, group I	Bulk					−193 ± 101		
Bulk Allende[d]		Bulk		1 ± 47	0.1 ± 1.2	−0.1 ± 1.9		−0.5 ± 3.2	−0.3 ± 4.5
CAI matrix test samples									
Synthetic CAI A	Synthetic CAI matrix + Te standard	Bulk		−414 ± 2092	22 ± 50	21 ± 74		23 ± 116	32 ± 162
Synthetic CAI B[c]	Synthetic CAI matrix + Te standard	Bulk		−2401 ± 2092	47 ± 50	52 ± 74		32 ± 116	
Synthetic CAI B[c]	Synthetic CAI matrix + Te standard	Bulk		−2636 ± 2092	46 ± 50	43 ± 74		8 ± 116	
USNM 3937 B	Matrix Fluffy Type A + Te standard	2 M HCl leach					2 ± 63		
USNM 3937 B	Matrix Fluffy Type A + Te standard	15 M HF leach		4307 ± 2598	−41 ± 40	−65 ± 81		−105 ± 149	−146 ± 217
USNM 3937 B	Matrix Fluffy Type A + Te standard	Steel bomb					16 ± 84		
Synthetic spectra[e]									
r-process excess Richter[f]				0	0	0	0	34	34
r-process excess Maas[g]				0	0	0	0	14	34
r-process excess Meyer[h]				0	7	0	−6	9	34
s-process depletion [i]				32	25	18	−7	33	34
r-process depletion Richter[f]				0	0	0	0	−34	−34
r-process depletion Maas[g]				0	0	0	0	−14	−34
r-process depletion Meyer[h]				0	−7	0	6	−9	−34
s-process excess[i]				−32	−25	−18	7	−33	−34
p-process excess[j]				5000	0	0	0	0	0

The quoted analytical uncertainties (2σ) include the errors for standard and sample measurements. Te isotopes were measured on Faraday collectors except ([a]), which were measured using electron multipliers.

$\varepsilon^{x}Te_{24} = \{[(^{x}Te/^{124}Te)_{sample} - (^{x}Te/^{124}Te)_{std}]/ (^{x}Te/^{124}Te)_{std}\} \times 10^4$, normalized to $^{122}Te/^{124}Te = 0.53594$ (Lee and Halliday 1995) with the exponential law; $\varepsilon^{126/125}Te_{M} = \{[(^{126}Te/^{125}Te)_{sample} - (^{126}Te/^{125}Te)_{std\ mean}]/ (^{126}Te/^{125}Te)_{std\ mean}\} \times 10^4$, calculated using the standard sample bracketing technique.

[b]No Xe interference correction was applied due to an interference on ^{129}Xe.

[c]Ba interference on ^{130}Te was too large for an accurate $\varepsilon^{130}Te_{24}$ measurement.

[d]From Fehr et al. (2004, 2005).

[e]Synthetic spectra are calculated assuming *r*-process compositions as determined by [f]Richter et al. (1998) and [g]Maas et al. (2001), and [h]as calculated by Meyer in Maas et al. (2001).

[i]*s*-process compositions are from Arlandini et al. (1999).

[j]A pure ^{120}Te *p*-process component is assumed.

Table 3. Te isotope data of Allende CAIs and CAI matrix test samples normalized to $^{125}Te/^{126}Te$.

Sample	Description	Leach/bulk	$\varepsilon^{120}Te_{56} \pm 2\sigma$	$\varepsilon^{122}Te_{56} \pm 2\sigma$	$\varepsilon^{124}Te_{56} \pm 2\sigma$	$\varepsilon^{128}Te_{56} \pm 2\sigma$	$\varepsilon^{130}Te_{56} \pm 2\sigma$
Allende CAIs							
USNM 3529 G[a]	Coarse-grained CAI, group I	Bulk	118 ± 270	−17 ± 11	−9.0 ± 6.3	7.1 ± 4.0	15.3 ± 7.6
USNM 3529 G	Coarse-grained CAI, group I	Bulk	−131 ± 235	−16 ± 22	−5 ± 13	7.0 ± 7.3	11 ± 15
USNM 3937 A	Several CAI's	HNO_3-Br leach	1080 ± 2588	18 ± 88	−2 ± 28	−12 ± 29	−23 ± 52
USNM 3937 B[b]	Fluffy Type A	15 M HF leach	177 ± 2562	17 ± 120	8 ± 35	−21 ± 50	
USNM 5171[a]	Coarse-grained CAI, group I	Bulk	127 ± 536	−48 ± 26	−17 ± 20	22 ± 14	43 ± 26
Bulk Allende[c]		Bulk	0 ± 49	−0.6 ± 2.1	−0.3 ± 1.1	0.0 ± 1.0	0.4 ± 2.0
CAI matrix test samples							
Synthetic CAI A	Synthetic CAI matrix + Te standard	Bulk	−436 ± 2054	−23 ± 117	−22 ± 53	2 ± 55	12 ± 106
Synthetic CAI B[b]	Synthetic CAI matrix + Te standard	Bulk	−2416 ± 2054	−31 ± 117	−42 ± 53	−30 ± 55	
Synthetic CAI B[b]	Synthetic CAI matrix + Te standard	Bulk	−2682 ± 2054	−57 ± 117	−50 ± 53	−28 ± 55	
USNM 3937 B	Matrix Fluffy Type A + Te standard	15 M HF leach	4191 ± 2562	−33 ± 120	17 ± 35	8 ± 50	13 ± 94
Synthetic spectra[d]							
r-process excess Richter[e]			0	0	0	34	34
r-process excess Maas[f]			0	0	0	14	34
r-process excess Meyer[g]			−40	−26	−13	21	59
s-process depletion[h]			−29	−46	−32	29	43
r-process depletion Richter[e]			0	0	0	−34	−34
r-process depletion Maas[f]			0	0	0	−14	−34
r-process depletion Meyer[g]			40	26	13	−21	−59
s-process excess [h]			29	46	32	−29	−43
p-process excess [i]			5000	0	0	0	0

The quoted analytical uncertainties (2σ) include the errors for standard and sample measurements. Te isotopes were measured on Faraday collectors.

$\varepsilon^{x}Te_{56} = \{[(^{x}Te/^{125}Te)_{sample} - (^{x}Te/^{125}Te)_{std}]/ (^{x}Te/^{125}Te)_{std}\} \times 10^4$, normalized to $^{125}Te/^{126}Te = 0.374902$ (Lee and Halliday 1995) with the exponential law.

[a]No Xe interference correction was applied due to an interference on ^{129}Xe.

[b]Ba interference on ^{130}Te was too large for an accurate $\varepsilon^{130}Te_{564}$ measurement.

[c]From Fehr et al. (2004, 2005).

[d]Synthetic spectra are calculated assuming r-process compositions as determined by [e]Richter et al. (1998) and [f]Maas et al. (2001), and [g]as calculated by Meyer in Maas et al. (2001).

[h]*s*-process compositions are from Arlandini et al. (1999).

[i]A pure ^{120}Te *p*-process component is assumed.

Table 4. Tin and Te concentrations of Allende CAIs.

	ppb Te	pg Te[a]	ppb Sn	$^{124}Sn/^{128}Te$
Coarse-grained CAI, USNM 3529 G				
Concentrated HF-HNO_3, bomb	365[b]		920[c]	0.5
Several CAIs, USNM 3937 A				
0.5 M HCl leach[d]	12–74[e]		157	0.4–2.3[e]
HNO_3-Br leach[d]	87–119[e]		140	0.2–0.3[e]
15 M HF leach[d]	109–171[e]		260	0.3–0.4[e]
Concentrated HF-HNO_3, bomb[d]	0–153[e]		12	>0.01[e]
Calculated bulk	307–537[e]		296	0.1–0.2[e]
Fluffy Type A CAI, USNM 3937 B				
2 M HCl leach		44		
15 M HF leach		245		
Concentrated HF-HNO_3, bomb		7		
Calculated bulk[b]	101			
Spinel-rich inclusion, USNM 3937 C				
2 M HCl leach		37		
15 M HF leach		39		
Concentrated HF-HNO_3, bomb		13		
Calculated bulk[b]	12			
Coarse-grained CAI, USNM 5171				
Concentrated HF-HNO_3, bomb	96[b]		1300[c]	2.5
Bulk Allende[f]	1034		543	0.1

[a]Amount of Te extracted from the sample after the chemical separation.
[b]Calculated from the amount of Te extracted from the sample after the chemical separation, assuming a yield of 70%.
[c]From Mason and Martin (1977).
[d]Concentrations relative to dissolved mass, which was approximated by the weight of the leachate solution, after evaporation to dryness.
[e]Sn/Te and Te concentration ranges represent zero to maximum possible Te blanks.
[f]From Fehr et al. (2005).

maximum possible blank. Tellurium concentration data and Sn/Te ratios are given in Table 4 as ranges that represent zero to maximum possible Te blanks. The maximum possible Te blank corresponds to 86 and 100% of the Te signals for the 0.5 M HCl leach fraction and the steel bomb digestion, respectively. For the HNO_3-Br and the 15 M HF leach, the Te blank corresponds to a maximum of 21 and 36% of the intensities.

The total blank for the Te separation procedure that was applied prior to isotopic analysis, was determined by MC-ICPMS with external calibration relative to Te standards of known concentration and using Nd or Cd as an internal standard to monitor non-spectral interferences. A similar procedure was applied to determine the Te concentrations of samples from which Te had been isolated by column chromatography. In the early stages of this project, during the processing of CAI sample USNM 3937 A (with ~1500 pg Te), the total procedural blank (digestion and Te chemical separation procedure) was relatively large at 30–400 pg Te, which is equivalent to a blank contribution of 5–25%. All further work was then carried out with a new set of Teflon vials and columns. This reduced the laboratory blank for Te isotope analyses to 0.6 pg Te and the blank contribution to <10%, given that the respective samples all had at least 5 pg Te.

RESULTS AND DISCUSSION

Tin and Tellurium Concentrations of CAIs

Calcium-aluminum rich inclusions feature a refractory mineralogy and they are thus thought to be the products of condensation of the cooling solar nebula (Grossman 1972; MacPherson et al. 1988) and melt evaporation (MacPherson et al. 2005). Tin and tellurium should therefore be highly depleted in these objects, as they are moderately volatile elements, with half mass condensation temperatures of 703 K and 705 K, respectively (Lodders 2003). Some studies, however, have reported relatively high abundances of moderately and highly volatile elements in CAIs (Grossman and Ganapathy 1976; Friedrich et al. 2005; Wombacher et al. 2008), and it has been suggested that this enrichment is the product of aqueous alteration (MacPherson 2003; Friedrich et al. 2005). Based on stable isotope data, however, it has also been proposed that the high Zn and Cd concentrations of

CAIs reflect interaction with and condensation of a gas phase, rich in metallic volatiles (Luck et al. 2005; Wombacher et al. 2008). Furthermore, relatively high concentrations of Te and Sn have also been reported for Fremdlinge (Armstrong et al. 1985), which are considered to be products of secondary alteration and sulfidization of primary metal grains in CAIs (MacPherson 2003).

Mason and Martin (1977) reported Sn concentrations of <50 to 7700 ppb for CAIs, and this corresponds to a maximum Sn enrichment or depletion of about an order of magnitude relative to bulk Allende, which has 543 ppb Sn (Fehr et al. 2005). Our result of 296 ppb Sn for sample USNM 3937 A (Table 4), which is a composite of several CAIs, is in accord with these previous data and it records a Sn depletion relative to bulk Allende of a factor of 2.

The Te content of the analyzed samples varies from 12 to 537 ppb Te, whereby the lowest value is recorded by the spinel rich inclusion USNM 3937 C (Table 4). These concentrations correspond to a Te depletion in CAIs relative to bulk Allende (1 ppm Te; Fehr et al. 2005) by factors of 2–3 (for the CAI composite USNM 3937 A) to 86. Most of these measurements have relatively large uncertainties, as sample size was limited.

Given that previous studies were unable to identify ^{126}Te isotope anomalies in bulk samples or leachates of various meteorites, including carbonaceous and ordinary chondrites as well as irons, it is essential that further investigations identify and focus on phases, which formed very early in the solar system and which have highly fractionated Sn/Te ratios. Sequential leaching of CAIs may reveal such phases, given that Te is a strongly chalcophile element, that can display siderophile behavior if no sulfides are present, whereas Sn is mainly siderophile with some chalcophile and lithophile tendencies. Spinels are also of interest because they are abundant in CAIs and are known to incorporate Sn into the crystal lattice (Bergerhoff et al. 1970), such that they may be characterized by particularly large Sn/Te ratios.

Bulk samples of Allende display ^{124}Sn/^{128}Te ≈ 0.1 but Allende leachates were found to exhibit significant fractionations of Sn from Te and ^{124}Sn/^{128}Te ratios of between 0.01 and 1.2 (Fehr et al. 2006). The CAIs analyzed in the present study display a similar range of ^{124}Sn/^{128}Te ratios, with values of 0.1 to 2.5 (Table 4). Both Allende leachates and CAIs are thus devoid of highly fractionated Sn/Te ratios. Such fractionations were also absent in the individual leachate fractions of the CAI sample USNM 3937 A (Table 4). For the latter sample, the largest ^{124}Sn/^{128}Te ratio was determined for the 0.5 M HCl leach (0.4–2.3), and moderate values (of 0.2–0.4) were obtained for the HNO_3-Br_2 and 15 M HF leachates. For the solution produced in the steel bomb digestion step (Table 4), which will have also attacked and dissolved any spinel originally present in the CAIs, it was possible to derive a lower limit for the ^{124}Sn/^{128}Te ratio of 0.01. This is because the maximum possible Te blank is equal to the Te content of this fraction. This leach fraction also contained only about 2% of the total Sn content of the inclusion, which suggests that the spinels had low Sn contents and did not contribute significantly to the total Sn budget of the CAI.

Precision and Accuracy of the Te Isotope Ratio Measurements

Analyses performed on 200 pg Te using Faraday detectors, internal normalization, and a time-resolved software display an external reproducibility of about ±2600 for $\varepsilon^{120}Te_{24}$ and $\varepsilon^{120}Te_{56}$, ±80 for $\varepsilon^{126}Te_{24}$, ±40 to ±220 for $\varepsilon^{125}Te_{24}$, $\varepsilon^{128}Te_{24}$ and $\varepsilon^{130}Te_{24}$, and ±35 to ±120 for $\varepsilon^{122}Te_{56}$, $\varepsilon^{124}Te_{56}$, $\varepsilon^{128}Te_{56}$ and $\varepsilon^{130}Te_{56}$. In contrast, 3 ng Te can be measured to a precision of about ±270 for $\varepsilon^{120}Te_{24}$ and $\varepsilon^{120}Te_{56}$, ±6 for $\varepsilon^{126}Te_{24}$, ±5 to ±18 for $\varepsilon^{125}Te_{24}$, $\varepsilon^{128}Te_{24}$ and $\varepsilon^{130}Te_{24}$, and ±4 to ±11 for $\varepsilon^{122}Te_{56}$, $\varepsilon^{124}Te_{56}$, $\varepsilon^{128}Te_{56}$ and $\varepsilon^{130}Te_{56}$. It was previously shown that internally normalized Te isotope data typically remain constant over time periods of several months and show no dependence on Te concentration (Fehr et al. 2006).

The external reproducibility (2s) for the $\varepsilon^{126/125}Te_M$ data collected with the electron multipliers is ~20 and ~150 ε-units, for analyses of about 65 and 3 pg of Te, respectively. Tellurium standard solutions with variable concentrations were analyzed using electron multipliers on six measurement sessions conducted over a period of five months. No difference in the $^{126/125}Te_M$ ratio is observed for 0.5 ppt–130 ppt Te standards measured on any particular day (Fig. 1). Small differences can be observed between different measurement sessions, which are probably related to variations in multiplier gain. The precision is not only dependent on the Te signal intensities (which vary with sensitivity and the concentration of Te), but is also highly dependent on the stability and magnitude of the background and, in particular, the Xe interferences. Accordingly, ^{125}Te was chosen as the numerator nuclide for these measurements because this has no isobaric overlap with Xe isotopes. In addition to these problems, drifts in the $^{126/125}Te_M$ ratio were observed during some measurement sessions and this worsens the reproducibility of the data.

The accuracy of the Te isotope measurements was evaluated using two synthetic CAI samples termed A and B. These samples consist of a mixture of quartz, calcite, dolomite, Al-foil, Fe, and Ti. These components were mixed in appropriate amounts to match the composition of 25 mg CAI material, and 1 ng of Te was then added. Further accuracy tests utilized the Te-free matrix fractions of USNM 3937 B, which were collected whilst solutions of the CAI leachates were processed through the primary anion-exchange column. These matrix fractions were dried down, doped with Te to match the original concentrations, and then further processed as normal samples.

The synthetic CAI samples show only very small deviations in ε^xTe_{24} and ε^xTe_{56} relative to the terrestrial

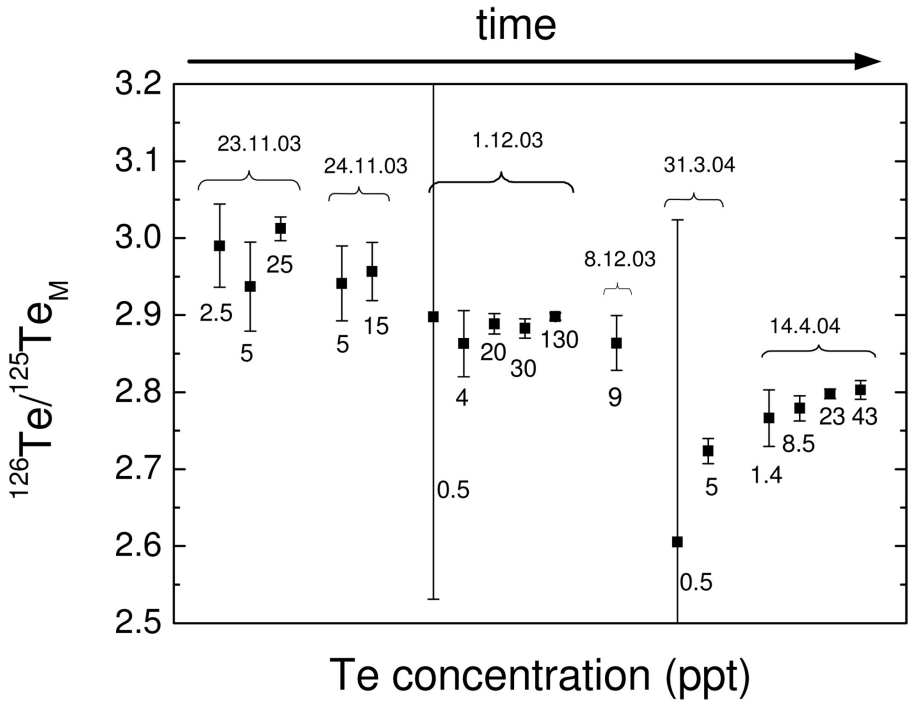

Fig. 1. Isotopic data ($^{126}Te/^{125}Te_M$) for Te standard solutions of different concentrations, measured using electron multipliers. Each data point represents the mean of 6–30 individual analyses. The quoted errors are 2σ external reproducibilities. The numbers denote the concentration of the Te standard in ppt and the date of the measurement (day.month.year).

standard (Table 2 and 3). The matrix test sample of the 15 M HF leach of USNM 3937 B is slightly high in $\varepsilon^{120}Te_{24}$ and $\varepsilon^{120}Te_{56}$ and low in $\varepsilon^{125}Te_{24}$ (Table 2 and 3) but the deviations from $\varepsilon^{x}Te = 0$ are only slightly larger than the quoted uncertainties. The $\varepsilon^{120}Te_{24}$ and $\varepsilon^{120}Te_{56}$ results for the synthetic CAI B are slightly negative but the offset is minor considering the large analytical uncertainty. All CAI matrix test samples furthermore have $\varepsilon^{126/125}Te_M$ values that are identical to the Te standard solution within uncertainties (Table 2).

No such accuracy tests were performed for the most precisely analyzed samples (USNM 3529 G and USNM 5171), as the matrix of these CAIs was saved for analyses of other isotope systems. However, all sample solutions were carefully checked for potential interfering elements that remained after the ion exchange separation. This involved tests, which determined whether the contaminant/Te ratio could compromise the Te isotope analyses. Significant amounts of Sr, Zr, Mo, Nb, Fe, Zn, Sn, and Ba were present in sample USNM 5171, but at levels too low to have an effect on the Te isotope measurements. Similar analyses revealed that the Zn, Ba, Fe, and Sn present in USNM 3539 G could not compromise the Te isotope data. However, it was noticed that the signal at mass 129, which was presumed to be from ^{129}Xe, was significantly larger for these two samples than for Te standard solutions. This is indicative of the presence of an unknown interference on mass 129, because the ^{129}Xe ion beam is generally very stable as Xe is a trace contaminant of the Ar plasma gas. The signal of ^{129}Xe is used for the correction of Xe interferences on masses 124, 126, 128, and 130. To avoid erroneous interference corrections, Xe-uncorrected data were used for samples USNM 3529 G, USNM 5171, and the corresponding Te standard measurements.

Taken together, these tests demonstrate that the Te isotope compositions of CAIs can be accurately determined to within the stated uncertainties using either Faraday cups (for samples with >100 pg Te) or electron multipliers (for <100 pg Te). Some minor deviations from the isotope composition of a pure Te standard solution were observed but these were always only slightly larger than the quoted uncertainties.

Tellurium Isotopic Compositions of CAIs

Variation in the Abundance of ^{126}Te and the Initial $^{126}Sn/^{124}Sn$ of the Solar System

All bulk CAIs and CAI leach fractions have $\varepsilon^{126}Te_{24}$ values that are identical within uncertainty to the Te standard and bulk Allende (Table 2 and Fig. 2). The most precise data, which was acquired with Faraday collectors, reveal no excesses in the abundance of ^{126}Te with $\varepsilon^{126}Te_{24}$ values of +1 ± 6 and −13 ± 24 for the coarse grained CAIs USNM 3529 G and USNM 5171, respectively. The electron multipliers analysis of USNM 5171 yielded slightly negative $\varepsilon^{126/125}Te_M$ values of −193 ± 101. The same sample solution was measured also using Faraday collectors. Conversely, these

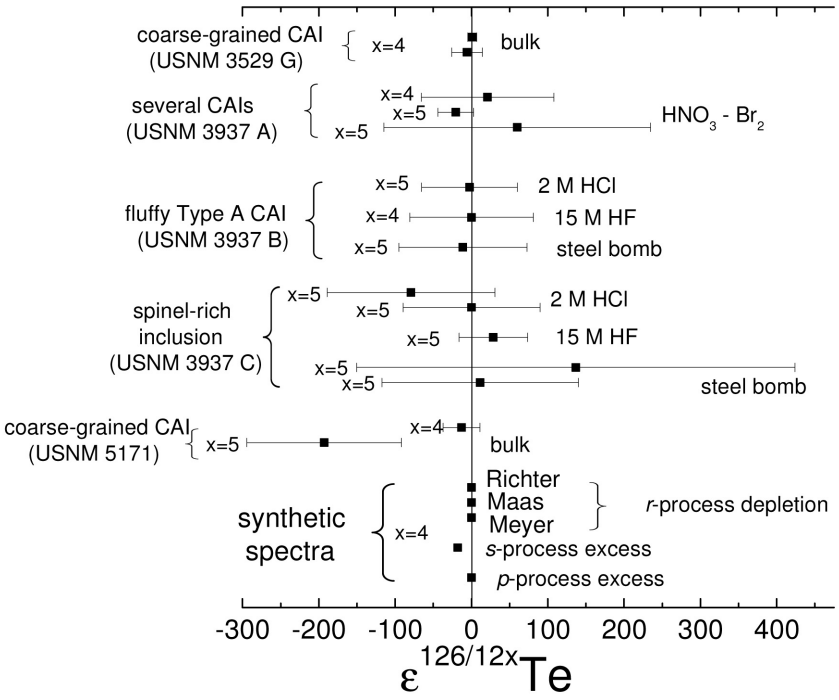

Fig. 2. $\varepsilon^{126/12x}$Te isotope results for Allende CAI samples. The error bars (2σ) represent the combined uncertainty of the sample and standard measurements. x = 5 represents $\varepsilon^{126/125}Te_M$, x = 4 represents $\varepsilon^{126}Te_{24}$, which is the $^{126}Te/^{124}Te$ isotope ratio normalized to $^{122}Te/^{124}Te = 0.53594$ (Lee and Halliday 1995) with the exponential law.

more precise data show no resolvable variations in the abundance of ^{126}Te and ^{125}Te with $\varepsilon^{126}Te_{24} = -13 \pm 24$ and $\varepsilon^{125}Te_{24}$ 2 ± 21. The coarse grained CAI USNM 5171 revealed the largest fractionation, with a $^{124}Sn/^{128}Te$ ratio of 2.5, whereas sample USNM 3529 G for which the most precise $\varepsilon^{126}Te_{24}$ data are available has a $^{124}Sn/^{128}Te$ ratio of 0.5 (Table 4).

There are presently no published supernova models that predict the nucleosynthetic productions yields of various isotopes relative to ^{126}Sn. The initial $^{126}Sn/^{124}Sn$ ratio of the solar system was estimated to be about $1–4 \times 10^{-5}$, as derived by Fehr et al. (2006) with the method of Meyer et al. (2004). This estimate is in agreement with published Te isotope data for sequential leachates of carbonaceous chondrites that yield a $^{126}Sn/^{124}Sn$ of $< 7.7 \times 10^{-5}$ at the time of closure of the Sn-Te system in the carrier phases (Fehr et al. 2006). Therefore, it should be possible to detect evidence for the former presence of live ^{126}Sn in early-formed materials, such as CAIs, with the presently available analytical techniques, if samples that exhibit high Sn/Te ratios could be investigated. However, only limited fractionation of Sn from Te was observed for the analyzed CAI samples, and this may be responsible for the absence of ^{126}Te excesses from the decay of the formerly live ^{126}Sn. Due to the low Sn/Te ratios in the investigated CAIs and the limited precision of the ε^{126}Te data, the new results are unable to provide improved constraints on the initial abundance of ^{126}Sn, and they only indicate an initial $^{126}Sn/^{124}Sn$ ratio of <0.0017.

The lack of positive ^{126}Te isotope anomalies implies that the free decay interval between the last supernova and the formation of the solar system may have been too long for sufficient amounts of ^{126}Sn to be incorporated into CAIs. In contrast, excesses in the abundance of ^{60}Ni from the decay of the short-lived radionuclide ^{60}Fe in USNM 3529G and USNM 5171 provide evidence for the presence of a short-lived radionuclide derived from a supernova source (Quitté et al. 2007). However, the ε^{60}Ni anomalies are relatively small (+0.6 and +1.1 ε units) and the half-life of ^{60}Fe (~1,490,000 yr) is about an order of magnitude larger compared to that of ^{126}Sn (234,500 yr). Quitté et al. (2007) showed that the ^{60}Ni anomalies were correlated with those of ^{62}Ni and argued that they therefore reflected variations in the amount of injected ^{60}Fe. Conversely, further analyses of the Fe-Ni system are needed to address uncertainties regarding the initial abundance of ^{60}Fe in the solar system (Dauphas et al. 2008; Regelous et al. 2008).

A number of recent studies have provided evidence for the former presence of live radioactive ^{41}Ca ($\tau_{½}$ ~103,000 yr) and ^{36}Cl ($\tau_{½}$ = 300,000 yr) in meteorites (Hutcheon et al. 1984; Srinivasan et al. 1994; Lin et al. 2005; Hsu et al. 2006; Nakashima et al. 2008). If these nuclides were mainly derived from a supernova source, then the free decay interval between nucleosynthetic production and the condensation of the first solids should have been short enough, in principle, for the incorporation of live ^{126}Sn into meteorites. A type-II supernova is able to generate a fresh supply of short-lived

isotopes, such as ^{26}Al, ^{41}Ca, ^{53}Mn, ^{60}Fe, and ^{107}Pd, even though very special conditions may be required to obtain initial abundances that are in accord with the published analytical data (Russell et al. 2001; Busso et al. 2003). However, ^{41}Ca can be produced in various stellar environments by both the *s*- and *r*-process (Meyer and Clayton 2000) as well as by spallation reactions (Lee et al. 1998; Leya et al. 2003).

Evidence for the extinct nuclide ^{41}Ca, which has an even shorter half-life than ^{126}Sn, has only been found in CAIs, where Ca is highly fractionated from the volatile daughter element K. High Ca/K ratios are present in particular in pyroxenes with ^{40}Ca/^{39}K ratios of up to 1×10^7 (Hutcheon et al. 1984; Srinivasan et al. 1994). The nuclide ^{36}Cl, which decays to ^{36}Ar and ^{36}S, has a half-life similar to that of ^{126}Sn. There is evidence for its former presence in sodalite and nepheline grains of CAIs with ^{35}Cl/^{34}S ratios as high as 6×10^4 (Lin et al. 2005). In contrast, the investigated samples displayed only limited enrichment of Sn relative to Te with ^{124}Sn/^{128}Te ratios of 0.1 to 2.5 (Table 4), which severely limits the amount of formerly live ^{126}Sn that can be detected. For comparison, estimates for the initial abundance of ^{41}Ca (^{41}Ca/^{40}Ca of ~1.4×10^{-8}, Srinivasan et al. 1996) and ^{36}Cl (^{36}Cl/^{35}Cl = 4–5 $\times 10^{-6}$, Lin et al. 2005; Hsu et al. 2006) from CAIs are slightly lower compared to those inferred for the initial solar system abundance of ^{126}Sn (^{126}Sn/^{124}Sn = 1–4 $\times 10^{-5}$). Furthermore, most Allende CAIs are substantially altered. It was proposed that this alteration could reflect either nebular or parent body processes (Krot et al. 1995; Fagan et al. 2004), whereas the parent body scenario is favored at present (e.g., Krot et al. 1998; Ford and Brearley 2008). This has implications for the interpretation of the Te isotope data, as Sn and Te may have been redistributed during alteration leading to a homogenization of the Te isotope compositions. However, evidence for the presence of the short-lived isotope ^{35}Cl was found even in alteration phases of CAIs (Lin et al. 2005). Conversely, the present study has investigated bulk CAIs that may have acted as an open system.

Nucleosynthetic Te Isotope Anomalies

All analyzed leach fractions and bulk CAIs have $\varepsilon^x Te_{24}$ values, which are within error identical to the terrestrial Te standard (Table 2, Fig. 3). The most precise analysis of USNM 3529 G displays an $\varepsilon^{125}Te_{24}$ value of +5.0 ± 5.2. This value cannot be interpreted as a nucleosynthetic isotope anomaly due to the uncertainty of the result. The analyses of USNM 5171 yielded values that are slightly low for $\varepsilon^{126}Te_{24}$ (−13 ± 24), $\varepsilon^{126/125}Te_M$ (−193 ± 101), $\varepsilon^{128}Te_{24}$ (−21 ± 39), and $\varepsilon^{130}Te_{24}$ (−30 ± 55), but the anomalies are either smaller than or do not greatly exceed the analytical uncertainties.

The data can be further evaluated considering the normalization scheme resulting in $\varepsilon^x Te_{56}$ values (Table 3), which typically have smaller uncertainties than the $\varepsilon^x Te_{24}$ values. In this case, the two most precise analyses of the coarse grained CAIs USNM 3529 G and USNM 5171 display small negative anomalies for $\varepsilon^{122}Te_{56}$ and $\varepsilon^{124}Te_{56}$ and small positive deviations for $\varepsilon^{128}Te_{56}$ and $\varepsilon^{130}Te_{56}$ (Fig. 4). These $\varepsilon^x Te_{56}$ results are significantly different from the terrestrial Te standard, although the anomalies are still small compared to the analytical uncertainties. The anomaly pattern shows good agreement with the synthetic spectra for *r*-process excesses and *s*-process deficits, as deduced from the theoretical calculations of Meyer in Maas et al. (2001) and Arlandini et al. (1999). This interpretation is in accord with the excesses of *r*-process Ni isotopes that were previously reported for these two inclusions (Quitté et al. 2007) and with Zr isotope data for other CAIs (Schönbächler et al. 2003).

Tests using synthetic CAI samples have shown that the presented ε^{120}Te data might be affected by small analytical artifacts (Table 2 and 3). Furthermore, there is a hint of an interference on ^{125}Te in the most precise analysis of USNM 3529 G ($\varepsilon^{125}Te_{24}$ of +5.0 ± 5.2), which would result in the observed anomaly pattern for $\varepsilon^x Te_{56}$. However, interferences on ^{125}Te from ^{111}Cd^{14}N, ^{85}Rb^{40}Ar and ^{109}Ag^{16}O can be excluded, as these elements are not present in the analyzed sample solution. Furthermore, the observed concentrations of Mo and Nb are also too low to account for the observed variations in ε^xTe. Additionally, the most precise analysis of USNM 5171, which displays the same anomaly pattern for $\varepsilon^x Te_{56}$ has a $\varepsilon^{125}Te_{24}$ of +2 ± 21 and this provides no evidence of an interference on ^{125}Te. Using ^{130}Te as the reference isotope and ^{130}Te/^{126}Te for mass-bias correction provides superior precision for the ε^{125}Te data. This gives positive $\varepsilon^{125}Te_{06}$ values of 10.8 ± 6.6 for USNM 5171 and +3.9 ± 1.9 for USNM 3529 G. However, positive $\varepsilon^{125}Te_{06}$ values would also be expected for *s*-process depletion and *r*-process excesses with *r*-process compositions as determined by Richter et al. (1998) and Maas et al. (2001). If the presented Te isotope data actually represent real nucleosynthetic isotope anomalies, it is unclear why they are considerably larger compared to anomalies for e.g., Ni and Zr (Schönbächler et al. 2003; Quitté et al. 2007). In summary, this indicates that the small observed Te isotope anomalies may hint at minor nucleosynthetic effects but analytical artifacts cannot be ruled out with confidence at present. Further investigations are therefore needed to clarify if the refractory inclusions indeed contain isotopically anomalous Te.

It has been suggested by Fujii et al. (2006a) that nuclear field shift effects could also be a cause of mass independent isotope variations in meteorites. The nuclear field shift theory also predicts anomalies for the tellurium isotope ^{125}Te (Fujii et al. 2006b) and therefore provides an alternative explanation for the small positive $\varepsilon^{125}Te_{24}$ value of +5.0 ± 5.2 that has been determined for CAI sample USNM 3529 G.

Many Allende CAIs harbor nucleosynthetic anomalies of various elements (Birck 2004; Harper Jr. 1993) and these anomalies are generally larger in the rare FUN (fractionated and unknown nuclear effects) inclusions. In normal Allende CAIs, nucleosynthetic isotope anomalies are absent for the relatively volatile elements Cd and Zn (Luck et al. 2005;

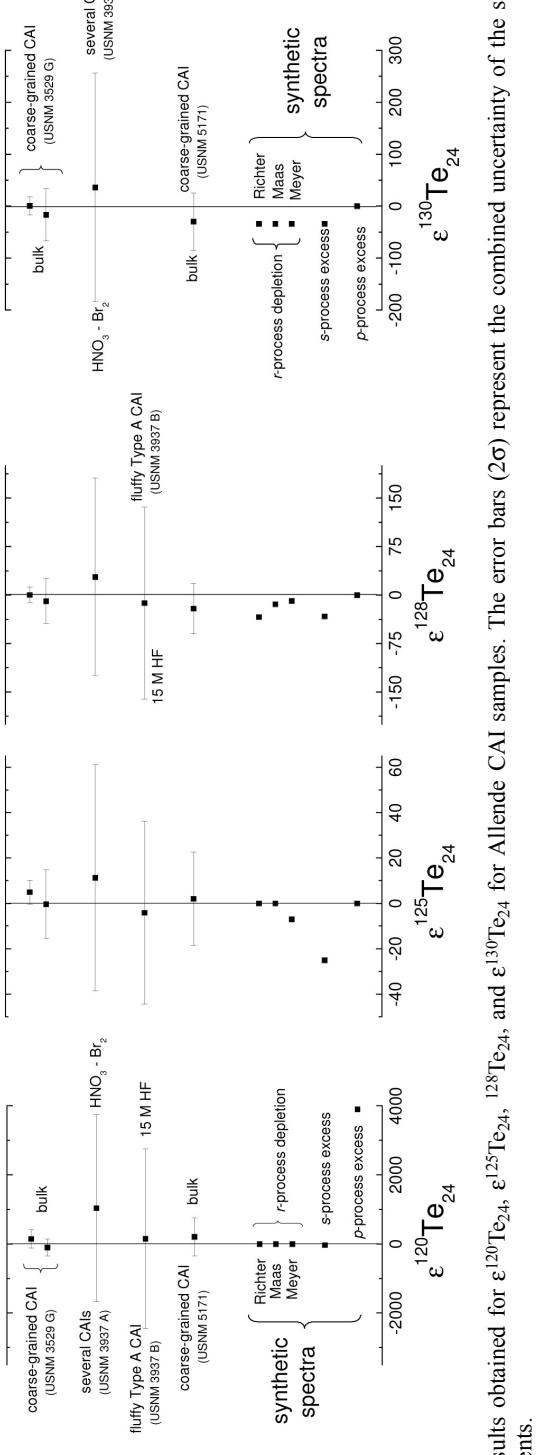

Fig. 3. Results obtained for $\varepsilon^{120}Te_{24}$, $\varepsilon^{125}Te_{24}$, $^{128}Te_{24}$, and $\varepsilon^{130}Te_{24}$ for Allende CAI samples. The error bars (2σ) represent the combined uncertainty of the sample and standard measurements.

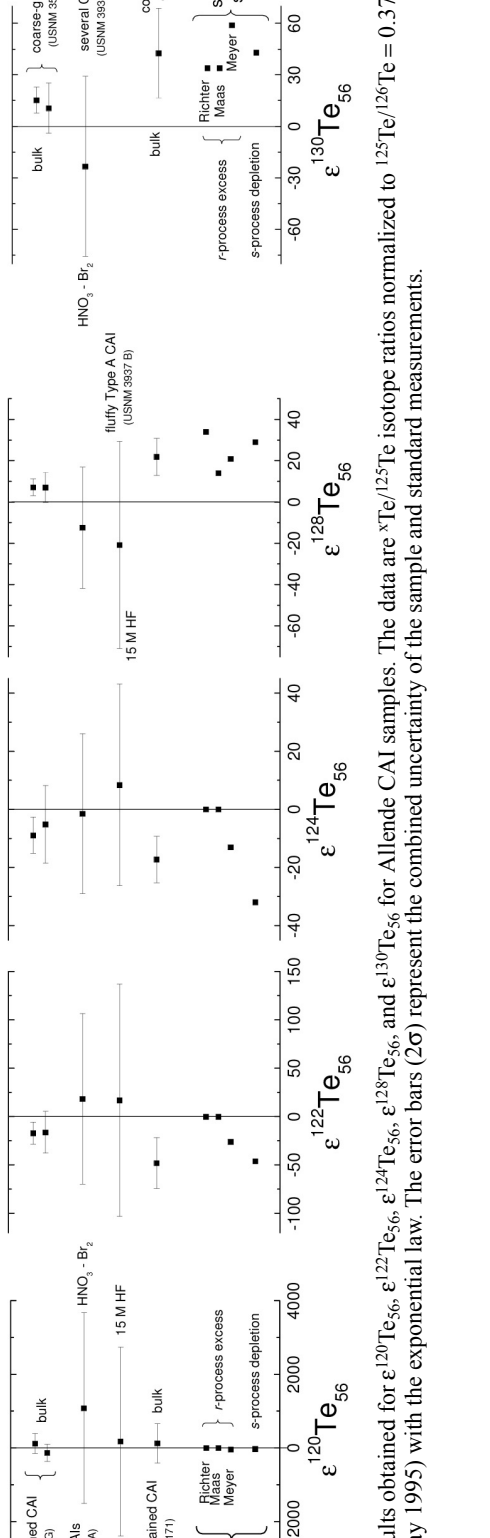

Fig. 4. Results obtained for $\varepsilon^{120}Te_{56}$, $\varepsilon^{122}Te_{56}$, $\varepsilon^{124}Te_{56}$, $\varepsilon^{128}Te_{56}$, and $\varepsilon^{130}Te_{56}$ for Allende CAI samples. The data are $^{x}Te/^{125}Te$ isotope ratios normalized to $^{125}Te/^{126}Te = 0.374902$ (Lee and Halliday 1995) with the exponential law. The error bars (2σ) represent the combined uncertainty of the sample and standard measurements.

Moynier et al. 2007; Wombacher et al. 2008) or they are at least smaller than the predictions of astrophysical models in the case of Zn (Loss and Lugmair 1990). Allende CAIs are generally more altered compared to CAIs from reduced CV chondrites (e.g., Krot 1995; Brearley 2003). It is therefore possible that existing anomalies were diluted by late-stage introduction of Te (and other elements) with a normal isotopic composition. Alternatively, the lack of anomalies may reflect homogenization of relatively volatile elements in the protosolar nebula (Kornacki and Wood 1985; Loss and Lugmair 1990). This is a reasonable explanation because the half mass condensation temperature of Te (709 K) is similar to that of Zn (723 K) and Cd (652 K) (Lodders 2003). The potential Te isotope anomalies of leachates from carbonaceous chondrites are also one to two orders of magnitude smaller than the effects observed for other more refractory elements, such as Mo or Zr, and this may be attributed to volatility-related homogenization as well (Fehr et al. 2006). Alternatively, it is conceivable that CAIs and chondrites have no or only minor nucleosynthetic isotope effects for relatively volatile elements, because the presolar carrier phases of these anomalies have very low contents of volatile constituents.

CONCLUSIONS

New methods were developed for the accurate and precise determination of Te isotopic compositions on pg to ng amounts of Te isolated from refractory inclusions of meteorites. Five CAIs from the CV3 carbonaceous chondrite Allende were investigated in this study. The Sn and Te concentrations of a composite sample that consists of several inclusions suggest that these elements are depleted in CAIs relative to bulk Allende by factors of about 2–3 and 3, respectively.

Tellurium isotope measurements of Allende CAIs revealed small potential nucleosynthetic Te isotope anomalies. However, further studies are needed to verify these results and exclude the possibility of analytical artifacts. Furthermore, the investigated refractory inclusions display no ^{126}Te excesses from the decay of ^{126}Sn. A comprehensive Te isotope study of refractory inclusions in combination with investigations of mineralogy and other short-lived radionuclide systems, such as ^{26}Al–^{26}Mg, could reveal whether the absence of radiogenic ^{126}Te anomalies in Allende CAIs is a general feature. In addition, such investigations may yield further constraints on whether the absence of positive ^{126}Te isotope effects reflects (1) the alteration of refractory inclusions, (2) the rather limited fractionation of Sn from Te, or (3) the lack of a supernova trigger or injection of short-lived radionuclides from a supernova into an already-formed protoplanetary disk after CAI formation. Further work should focus on Te isotope analyses of CAIs with high Sn concentrations and on samples that show less secondary processing. In this respect it is important to have a better understanding of the distribution of Sn and Te in the phases of bulk meteorites and CAIs in order to identify primary minerals with high Sn/Te ratios. Such phases have the best chance of hosting radiogenic ^{126}Te isotope anomalies.

Acknowledgments—We thank Der-Chuen Lee, Glenn MacPherson, Don Porcelli, Maria Schönbächler, Uwe Wiechert, Sarah Woodland, and Brigitte Zanda for many helpful discussions. Glenn MacPherson is furthermore acknowledged for providing samples USNM 3529 G, USNM 3937 and USNM 5171 from the meteorite collection at the Smithsonian Institution of Washington. Moreover, we are grateful to Glenn MacPherson and Nadia Vogel for initial help with the separation and characterization of CAIs. We also would like to thank Claudine Stirling and Morten Andersen for their introduction to and discussions of the use of electron multipliers for isotopic analysis. Frederic Moynier and an anonymous reviewer are acknowledged for their constructive reviews. Furthermore, Adrian Brearley is thanked for his comments on the manuscript and the editorial work. Financial support was provided by the ETH Forschungskomission and the Schweizerische Nationalfonds (SNF). Alex Halliday acknowledges support from the Royal Society and STFC.

Editorial Handling—Dr. Adrian Brearley

REFERENCES

Amelin Y., Krot A. N., Hutcheon I. D., and Ulyanov A. A. 2002. Lead isotopic ages of chondrules and calcium-aluminum-rich inclusions. *Science* 297:1678–1683.

Arlandini C., Käppeler F., and Wisshak K. 1999. Neutron capture in low-mass asymptotic giant branch stars: Cross sections and abundance signatures. *The Astrophysical Journal* 525:886–900.

Armstrong J. T., Hutcheon I. D., and Wasserburg G. J. 1985. Ni-Pt-Ge-rich Fremdlinge: Indications of a turbulent early solar nebula (abstract). *Meteoritics* 20:603–604.

Bergerhoff G., Hamaguchi H., Kuroda R., and Wedepohl K. H. 1970. 50. Tin. In *Handbook of geochemistry*, edited by Wedepohl K. H. New York: Springer Verlag.

Birck J. L. 2004. An overview of isotopic anomalies in extraterrestrial materials and their nucleosynthetic heritage. In *Geochemistry of non-traditional stable isotopes*, edited by Johnson C. M., Beard B. L., and Albarède F. Washington D.C.: The Mineralogical Society of America. pp. 25–64.

Bouvier A., Blichert-Toft J., Moynier F., Vervoort J., and Albarède F. 2007. New Pb-Pb ages relevant to the accretion and cooling history of chondrites. *Geochimica et Cosmochimica Acta* 71: 1583–1604.

Brearley A. J. 2003. Nebular versus parent-body processing. In *Meteorites, comets, and planets*, edited by Davis A. Treatise on Geochemistry, vol. 1. Amsterdam: Elsevier.pp. 201–247.

Busso M., Gallino R., and Wasserburg G. J. 2003. Short-lived nuclei in the early solar system: A low mass stellar source? *Publications of the Astronomical Society of Australia* 20:356–370.

Cameron A. G. W. and Truran J. W. 1977. The supernova trigger for formation of the solar system. *Icarus* 30:447–461.

Chevalier R. A. 2000. Young circumstellar disks near evolved massive stars and supernovae. *The Astrophysical Journal* 538: L151–L154.

Dauphas N., Cook D. L., Sacarabany A., Fröhlich C., Davis A. M., Wadhwa M., Pourmand A., Rauscher T., and Gallino R. 2008. Iron-60 evidence for early injection and efficient mixing of stellar debris in the protosolar nebula. *The Astrophysical Journal* 686: 560–569.

Fagan T. J., Krot A. N., Keil K., and Yurimoto H. 2004. Oxygen isotopic alteration in Ca-Al-rich inclusions from Efremovka: Nebular or parent body setting? *Meteoritics & Planetary Science* 39:1257–1272.

Fehr M. A., Rehkämper M., and Halliday A. N. 2004. Application of MC-ICPMS to the precise determination of tellurium isotope compositions in chondrites, iron meteorites and sulfides. *International Journal of Mass Spectrometry* 232:83–94.

Fehr M. A., Rehkämper M., Halliday A. N., Wiechert U., Hattendorf B., Günther D., Ono S., and Rumble III D. 2005. The tellurium isotopic composition of the early solar system—A search for isotope anomalies from the decay of ^{126}Sn, stellar nucleosynthesis, and mass independent fractionations. *Geochimica et Cosmochimica Acta* 69:5099–5112.

Fehr M. A., Rehkämper M., Halliday A. N., Schönbächler M., Hattendorf B., and Günther D. 2006. Search for nucleosynthetic and radiogenic tellurium isotope anomalies in carbonaceous chondrites. *Geochimica et Cosmochimica Acta* 70:3436–3448.

Ford R. L. and Brearley A. J. 2008. Element exchange between matrix and CAIs in the Allende meteorite (abstract #2399). 39th Lunar and Planetary Science Conference. CD-ROM.

Friedrich J. M., Jochum K. P., and Ebel D. S. 2005. Elemental signatures of nebular and alteration processes in CV, CO, and CR CAI´s (abstract). *Meteoritics & Planetary Science* 40:A51.

Fujii T., Moynier F., and Albarède F. 2006b. Mass-independent isotope fractionation of Mo, Ru, Cd, and Te (abstract #V21B-0571). *Eos Transactions*, American Geophysical Union, Fall Meeting Supplement 87.

Fujii T., Moynier F., and Albarède F. 2006a. Nuclear field versus nucleosynthetic effects as cause of isotopic anomalies in the early solar system. *Earth and Planetary Science Letters* 247:1–9.

Göpel C., Manhès G., and Allègre C. J. 1994. U-Pb systematics of phosphates from equilibrated ordinary chondrites. *Earth and Planetary Science Letters* 121:153–171.

Grossman L. 1972. Condensation in the primitive solar nebula. *Geochimica et Cosmochimica Acta* 36:597–619.

Grossman L. and Ganapathy R. 1976. Trace elements in the Allende meteorite-II. fine-grained, Ca-rich inclusions. *Geochimica et Cosmochimica Acta* 40:967–977.

Harper Jr. C. L. 1993. Isotopic astronomy from anomalies in meteorites: Recent advances and new frontiers. *Journal of Physics G: Nuclear and Particle Physics* 19:S81–S94.

Hsu W., Guan Y., Leshin L. A., Ushikubo T., and Wasserburg G. J. 2006. A late episode of irradiation in the early solar system: Evidence from extinct ^{36}Cl and ^{26}Al in meteorites. *The Astrophysical Journal* 640:525–529.

Hutcheon I. D., Armstrong J. T., and Wasserburg G. J. 1984. Excess ^{41}K in Allende CAI: Confirmation of a hint (abstract). 15th Lunar and Planetary Science Conference. pp. 387–388.

Jacobsen B., Yin Q.-Z., Moynier F., Amelin A., Krot A. N., Nagashima K., Hutcheon I. D., and Palme H. 2008. ^{26}Al–^{26}Mg and ^{207}Pb–^{206}Pb systematics of Allende CAIs: Canonical solar initial ^{26}Al/^{27}Al ratio reinstated. *Earth and Planetary Science Letters* 272:353–364.

Kornacki A. S. and Wood J. A. 1985. Mineral chemistry and origin of spinel-rich inclusions in the Allende CV3 chondrite. *Geochimica et Cosmochimica Acta* 49:1219–1237.

Krot A. N., Scott E. R. D., and Zolensky M. E. 1995. Mineralogical and chemical modification of components in CV3 chondrites: Nebular or asteroidal processing? *Meteoritics* 30:748–775.

Krot A. N., Petaev M. I., Scott E. R. D., Choi B.–H., Zolensky M. E., and Keil K. 1998. Progressive alteration in CV3 chondrites: More evidence for asteroidal alteration. *Meteoritics & Planetary Science* 33:1065–1085.

Lee D.-C. and Halliday A. N. 1995. Precise determinations of the isotopic compositions and atomic weights of molybdenum, tellurium, tin and tungsten using ICP magnetic sector multiple collector mass spectrometry. *International Journal of Mass Spectrometry and Ion Processes* 146/147:35–46.

Lee T., Shu F. H., Shang H., Glassgold A. E., and Rehm K. E. 1998. Protostellar cosmic rays and extinct radioactivities in meteorites. *The Astrophysical Journal* 506:898–912.

Leya I., Halliday A. N., and Wieler R. 2003. The predictable collateral consequences of nucleosynthesis by spallation reactions in the early solar system. *The Astrophysical Journal* 594:605–616.

Lin Y. T., Guan Y. B., Leshin L. A., Quayang Z. Y., and Wang D. 2005. Short-lived chlorine-36 in a Ca- and Al-rich inclusion from the Ningqiang carbonaceous chondrite. *Proceedings of the National Academy of Sciences* 102:1306–1311.

Lodders K. 2003. Solar system abundances and condensation temperatures of the elements. *The Astrophysical Journal* 591: 1220–1247.

Loss R. D. and Lugmair G. W. 1990. Zinc isotope anomalies in Allende meteorite inclusions. *The Astrophysical Journal* 360: L59–L62.

Luck J.-M., Ben Othman D., and Albarède F. 2005. Zn and Cu isotopic variations in chondrites and iron meteorites: Early solar nebula reservoirs and parent-body processes. *Geochimica et Cosmochimica Acta* 69:5351–5363.

Maas R., Loss R. D., Rosman K. J. R., De Laeter J. R., Lewis R. S., Huss G. R., and Lugmair G. W. 2001. Isotope anomalies in tellurium and palladium from Allende nanodiamonds. *Meteoritics & Planetary Science* 36:849–858.

MacPherson G. J. 2003. Calcium-aluminium-rich inclusions in chondritic meteorites. In *Meteorites, comets, and planets*, edited by Davis A. Amsterdam: Elsevier. Treatise on Geochemistry, vol. 1. pp. 201–247.

MacPherson G. J., Simon S. B., Davis A. M., Grossman L., and Krot A. N. 2005. Calcium-aluminum-rich inclusions: Major unanswered questions. In *Chondrites and the Protoplanetary Disk*, edited by Krot A. N., Scott E. R. D., and Reipurth B. ASP Conference Series 341. pp. 225–250.

MacPherson G. J., Wark D. A., and Armstrong J. T. 1988. Primitive material surviving in chondrites: Refractory inclusions. In *Meteorites and the early solar system*, edited by Kerridge J. F. and Matthews M. S. Tucson: The University of Arizona Press. pp. 746–807.

Mason B. and Martin P. M. 1977. Geochemical differences among components of the Allende meteorite. *Smithsonian Contributions to the Earth Sciences* 19:84–95.

McKeegan K. D. and Davis A. M. 2003. Early solar system chronology. In *Meteorites, comets, and planets*, edited by Davis A. Amsterdam: Elsevier. Treatise on Geochemistry, vol. 1. pp. 431–461.

Meyer B. S. and Clayton D. D. 2000. Short-lived radioactivities and the birth of the sun. *Space Science Reviews* 92:133–152.

Meyer B. S., The L.-S., and Clayton D. D. 2004. Helium-shell nucleosynthesis and extinct radioactivities (abstract #1908). 35th Lunar and Planetary Science Conference. CD-ROM.

Moynier F., Blichert-Toft J., Luck J. M., Telouk P., and Albarède F. 2007. Comparative stable isotope geochemistry of Ni, Cu, Zn, and Fe in chondrites and iron meteorites. *Geochimica et Cosmochimica Acta* 71:4365–4379.

Nakashima D., Ott U., Hoppe P., and El Goresy A. 2008. Search for extinct ^{36}Cl: Vigarano CAIs, the Pink Angel from Allende, and a Ningqiang chondrule. *Geochimica et Cosmochimica Acta* 72: 6141–6153.

Oberli F., Gartenmann P., Meier M., Kutschera W., Suter M., and Winkler G. 1999. The half-life of ^{126}Sn refined by thermal ionization mass spectrometry measurements. *International Journal of Mass Spectrometry* 184:145–152.

Ouellette N., Desch S. J., Hester J. J., and Leshin L. A. 2005. A nearby supernova injected short-lived radionuclides into our protoplanetary disk. In *Chondrites and the Protoplanetary Disk*, edited by Hewins R. H., Jones R. H., and Scott E. R. D. Cambridge University press. pp. 527–538.

Podosek F. A. and Swindle T. D. 1988. Extinct Radionuclides. In *Meteorites and the early solar system*, edited by Kerridge J. F. and Matthews M. S. Tucson: The University of Arizona Press. pp. 1093–1113.

Qian Y.-Z., Vogel P., and Wasserburg G. J. 1998. Supernova as the site of the r-process: Implications for gamma-ray astronomy. *The Astrophysical Journal* 506:868–873.

Quitté G., Halliday A. N., Meyer B. S., Markowski A., Latkoczy C., and Günther D. 2007. Correlated iron 60, nickel 62, and zirconium 96 in refractory inclusions and the origin of the solar system. *The Astrophysical Journal* 655:678–684.

Regelous M., Elliott T., and Coath C. D. 2008 Nickel isotope heterogeneity in the early solar system. *Earth and Planetary Science Letters* 272: 330–228.

Rehkämper M. and Halliday A. N. 1999. The precise measurement of Tl isotopic compositions by MC-ICPMS: Application to the analysis of geological materials and meteorites. *Geochimica et Cosmochimica Acta* 63:935–944.

Richter S., Ott U., and Begemann F. 1998. Tellurium in pre-solar diamonds as an indicator for rapid separation of supernova ejecta. *Nature* 391:261–263.

Russell S. S., Gounelle M., and Hutchinson R. 2001. Origin of short-lived radionuclides. *Philosophical Transactions: Mathematical, Physical and Engineering Sciences* 359:1991–2004.

Schönbächler M., Lee D.-C., Rehkämper M., Halliday A. N., Fehr M. A., Hattendorf B., and Günther D. 2003. Zirconium isotope evidence for incomplete admixing of *r*-process components in the solar nebula. *Earth and Planetary Science Letters* 216:467–481.

Srinivasan G., Ulyanov A. A., and Goswami J. N. 1994. ^{41}Ca in the early solar system. *The Astrophysical Journal* 431:L67–L70.

Srinivasan G., Sahijpal S., Ulyanov A. A., and Goswami J. N. 1996. Ion microprobe studies of Efremovka CAIs: II. Potassium isotope composition and ^{41}Ca in the early solar system. *Geochimica et Cosmochimica Acta* 60:1828–1835.

Wombacher F., Rehkämper M., Mezger K., Bischoff A., and Münker C. 2008. Cadmium stable isotope cosmochemistry. *Geochimica et Cosmochimica Acta* 72:646–667.